Petroleum and Coal

Article **Open Access**

Performance Enhancement of Graphene Nano-sheets Supported Cobalt Fischer–Tropsch Synthesis Catalysts via Support Functionalization

Iraj Kazemnejad[1], Alireza Feaizbakhsh[1], Ali Niazi[1], Ahmad Tavasoli[2]*

[1] Department of Chemistry, Central Tehran Branch, Islamic Azad University, Tehran, Iran
[2] School of Chemistry, College of Science, University of Tehran, Tehran, Iran

Received October 13, 2021, Accepted March 1, 2022

Abstract

Graphene nano sheets (GNS) and functionalized GNS was used as support for cobalt catalyst in Fischer-Tropsch synthesis (FTS). A fixed bed micro-reactor was used to investigate the activity, stability and selectivity of cobalt catalyst supported on GNS and functionalized GNS. Chemical vapor deposition (CVD) technique was used to load cobalt on the surface of the supports. Pysico-chemical characteristics of supports and fresh and used catalysts were studied by FTIR, XRD, TPR, TEM, Raman spectroscopy and H_2 chemisorption techniques. Functionalization decreased the average cobalt particles size from 7.8 to 6.8 nm, increased the % dispersion from 23.7 to 27.2 and increased the catalyst reducibility by 15%. Also, percentage CO conversion increased from 78.4 to 84.9%. Functionalized catalyst showed better stability.

Graphene nano sheets (GNS) were functionalized and used as cobalt Fischer–Tropsch synthesis (FTS) catalyst support. The effects of nitrogen functional groups on graphene surface on the activity, selectivity and stability of cobalt catalyst in FTS was investigated using a fixed bed micro-reactor. 15 wt.% of cobalt was loaded on the supports by impregnation method. Physico-chemical properties of pure and functionalized graphene, calcined fresh and used catalysts were studied by Raman spectroscopy, FTIR, BET, XRD, TEM, TPR and H2chemisorption techniques. According to the TEM and H2chemisorption tests, 480 hrs continuous FT synthesis increased the average cobalt particle size from about 7.8 to 8.8 nm for Co/GNS catalyst and from about 6.8 to 7.2 nm for Co/N-GNS catalyst. The proposed cobalt catalyst supported on functionalized GNS increased the initial %CO conversion from 70.6 to 74.5. The CO conversion over the Co/N-GNS after 480 hrs on stream decreased by 4.3% and that for Co/GNS decreased by 6.2%. For the Co/N-GNS catalyst 0.6% of total activity loss and for the Co/GNS catalyst 3.1% of total activity loss cannot be recovered after regeneration of the catalyst at the same conditions of the first regeneration step.Catalysts supported on functionalized GNS showed better stability.

***Keywords**: Graphene nano sheets; Cobalt; Functionalization; Activity; Selectivity; Stability.*

1. Introduction

Processing of fossil fuels with a sustainable and efficient method could be a key solution to control the harmful environmental effects of greenhouse gases emission. Liquid fuels derived from Fischer-Tropsch synthesis (FTS) of natural gas are a clean option with several beneficial properties compared with some conventional fossil fuels. These properties are including low level amounts of aromatics in the fuel, zero sulfur and nitrogen. Potentially, FTS is a promising alternative for environmentally friendly fuels and some chemicals from biomass, coal and natural gas. In industrial scale, catalysts with a high performance can play a critical role. In this process, selectivity, activity and lifetime of the catalysts are under effect of many different factors including structure and nature of the support, metal, metal dispersion, metal loading and catalysts preparation procedure. Because of economically high selectivity and activity of cobalt catalysts, they are mainly used in the low temperature FTS. Recently, researchers have focused on the improving catalysts activity, stability and selectivity. The potential factors for catalysts deactivation of cobalt-based FTS are re-oxidation of cobalt, sintering, formation of

some stable species in the layer between cobalt and support, poisoning, carbiding and formation of carbon-based materials on the cobalt surface. Carbon-based nanomaterials have been widely used in different areas as a useful material in order to enhance the efficiency of the processes. Their high surface area, thermal stability, recyclability and tensile strength are important and interesting factors leading to considering them as key materials in chemistry related processes. Cobalt is considered as the most applicable metal for synthesis of long chain hydrocarbons due to its low water-gas shift activity and high selectivity to linear paraffins. The catalyst is usually dispersed on an oxide support. Also, Co catalysts supported on carbon nanotubes have been widely used in FTS. Graphene is currently a support key material in heterogeneous catalysis systems because of its unique characteristics including well developed porosity, high intrinsic carrier, thermal stability and some electronic and mechanic properties. Also, graphene is inert and has hydrophobic nature. The interaction between the support surface and active metal is a key point in catalysis. Poor and strong interaction with the metal particles leads to agglomeration and stabilization of the supported nanoparticle, respectively.

It seems that functionalization of graphene by nitrogen containing materials and producing N-functionalized graphene, the location of the cobalt metal will be more probable on the top of nitrogen atoms present in the structure of the graphene rather than that of carbon atoms. So, the stabilization of cobalt on functionalized graphene will be better due to the interaction between metal and N atoms available in the structure. In present study, graphene was functionalized by nitrogen groups before loading of cobalt precursors and the performance of Co/GNS and Co/N-GNS catalysts was evaluated in a fixed bed micro reactor. The main focus is to investigate catalysts prepared by chemical vapor deposition (CVD) technique on different promising supports to have the further insights into the CVD approach which could lead to emerging a new and scalable method for preparing the next generation of Co catalysts.

2. Experimental

2.1.Support preparation

2.1.1. Preparation and purification of graphene

The graphene was prepared according to the modified Hummer method. In brief, 8 g graphite powder, 4 g sodium nitrate, and 100 ml concentrated sulphuric acid and 12 mL phosphoric acid was added to a container under stirring for 15 min in an ice bath. Then, 16 g KMnO4 was slowly added to the solution and stirred for 10 min to obtain a solution. The mixture was under heating condition to desired temperature within the range of 35-40°C. After half an hour and obtaining a thickened mixture, 240 mL deionized water was slowly added to the mixture and stirred for 20 min. An excessive 700 mL of water was added followed by the slow addition of 50 mL H_2O_2 (30%). Afterward, the mixture was centrifuged and washed with deionized water and 5% HCl to remove any impurities from the suspension. Finally, the suspension was dried at 60°C to obtain a powder. The support was called as GNS.

2.1.2. Functionalization of GNS

300 mg of the sample was added to ethylene glycol and the solution was maintained under ultrasonication condition and then 2 mL of ammonia water was added. The as-prepared dark brown solution was transferred to an autoclave (Teflon) to react solvo-thermally at 220°C for 10 h. After the time that reaction was completed, the precipitate was filtered and washed with distilled water for several times. The precipitate was dried at 70°C for 24 h. The support was called as N-GNS.

2.2. Preparation of catalyst by CVD method

Certain amounts of cobalt acetylacetonates ($Co(acac)_2$ Alfa Aesar) and support (GNS and N-GNS) were loaded into a sublimation tube that was sealed and connected to a vacuum system. The sublimation tube was slowly ramped to 100°C, and maintained at this temperature for 2h. Then the temperature was increased to 130°C and maintained at this temperature for 2 h. Argon was used as the carrier gas. Decomposing of the cobalt acetylacetonate

$Co(acac)_2$ compound was conducted in flowing argon for 4 h at 350°C. The catalysts prepared by CVD method were named as Co/GNS and Co/N-GNS.

2.3. Catalyst characterization

The FTIR technique was performed on a Bruker ISS-88. For each adsorption measurement 0.5–5% of samples mixed with 95–99.5% potassium bromide (KBr) and a transparent pellet was prepared and the infrared beam passed through pellets. A Confocal Raman Microscope System with a laser source of 785 nm was used to measure the Raman shift of the support materials.

Field-emission scanning electron microscopy (FESEM JEOL-JSM-6700F instrument) was performed on prepared catalysts to analyze the morphology and homogeneity of Co particles. The samples were prepared by dispersing catalyst powder onto a carbon-coated copper grid.

BET surface area measurements were carried out using an ASAP-2010 system from Micrometrics. In each trial, a weight of approximately 0.25 g of sample was degassed at 200°C for 4h under 50 mTorr vacuum and the BET area, pore volume, and average pore radius were determined.

Cobalt loadings were measured using a Varian VISTA-MPX Inductively Coupled Plasma Atomic Emission Spectroscopy (ICP-AES) system. The mixture including 0.02 g of the catalyst sample in 5 ml of nitric acid (Merck 65%) and 5 ml hydrochloric acid (Chem-Lab, 37%) stirred at 40–50°C for 2 h was filtered and then diluted up to 250 mL.

The phases and crystallite sizes of the catalysts was studied using XRD. A Philips analytical X-ray diffractometer (XPert MPD) with monochromatized Cu/Kα radiation, 2θ angles from 20 to 80° recorded the patterns. The crystal size of the Co_3O_4 was calculated using the Scherrer's equation (2θ = 36.8°).

Micrometrics TPD–TPR 2900 system was equipped with a thermal conductivity detector (TCD) to conduct H_2-TPR. Little amounts of water and gases were removed from the catalysts by purging a flow of Helium at 140°C. After reaching to 40°C by cooling, TPR of the samples was obtained using 5% H_2 in Ar stream at a flow rate of 40 mL/min and atmospheric pressure and a linearly programmed heating (10°C/min) up to 850°C.

Metal dispersion and the average active surface area were evaluated using the TPD technique. First the TPD of hydrogen was conducted and then pulses of 10% oxygen in helium were entered to re-oxidize the samples at 400°C and the extent of reduction was determined. It is to note that during re-oxidation step GNS has not reacted with oxygen which was clear from the absence of CO_2 peak. It was assumed that Co° was oxidized to Co_3O_4. The calculations are summarized below [1].

$$\%Dispersion = \frac{number\ of\ Co^0 atoms\ on\ surface}{number\ of\ Co\ atoms\ in\ sample} \times 100$$

$$Fraction\ reduced = \frac{O_2\ Uptake\left(\frac{molO2}{grcatalyst}\right) \times \frac{2}{3} \times Cobalt\ atomic\ weight(58.9332 gr/mol)}{Percentage\ metal}$$

$$d(nm) = \frac{6000}{Density \times maximum\ area \times dispersion}$$

2.4. Catalyst activity experiments

Catalysts performance in FTS was studied in a fixed bed reactor. The reactor temperature was fixed at desired temperature using an internal K type thermocouple and a PID temperature controller. 0.6 g of catalyst was diluted with 2.4 gr silicon carbide and used on catalytic tests. Brooks 5850 mass flow controllers where used to inject hydrogen and carbon monoxide to the reaction system. After in-situ reduction of the catalyst at 400°C and H_2=30 mL/min for 18 h, the reactor temperature decreased and FT tests were conducted at 220°C, 1.8 MPa, H_2/CO=2 and a total flow rate of 45mL/min. Products were removed and passed through two traps, a hot trap (at 100°C) and a cold trap (at 0°C). The uncondensed vapor pressure was reduced to atmospheric conditions. The out let gas flow was measured using a bubble flow meter, analyzed by an online GC and used to measure the CO conversion and gaseous products selectivities. The accumulated liquid (wax, oil and aqueous) products were removed every 24 h and analyzed by GC.

3. Results and discussion

3.1. Graphene characterization

The FTIR spectra of purified and functionalized graphene are presented in Fig. 1. The featured peaks at 1575 cm^{-1} and 1578 cm^{-1} observed for GNS and N-GNS are corresponded to the stretching mode of double-bonds (C=C) in the structure of graphene. The coupling of functional groups to graphene can be verified with a series of new vibrational bands at 3300–3600 cm^{-1} (OH). Peaks observed at 1790 cm^{-1} (C=O) are related to carboxyl groups, 1165 cm^{-1} (C-O), 2850–2950 cm^{-1} both are attributed to C-H anti symmetric and symmetric stretch for CH_3 and CH_2. The peak at 615 cm^{-1} is arising from the bands of C-H bending mode. The main reason for this peak is the defects left by well-functionalization of graphene. In addition, in spectrum of N-GNS new peaks appeared. The peak at 1020 cm^{-1} is related to the C-N stretching frequency. The broadening peak at 3300–3400 cm^{-1} significantly verifies the NH stretching frequency. A shift in C=O stretching frequency from 1790 cm^{-1} in GNS to 1714 cm^{-1} in N-GNS verifies the presence of NH bonds in the structure.

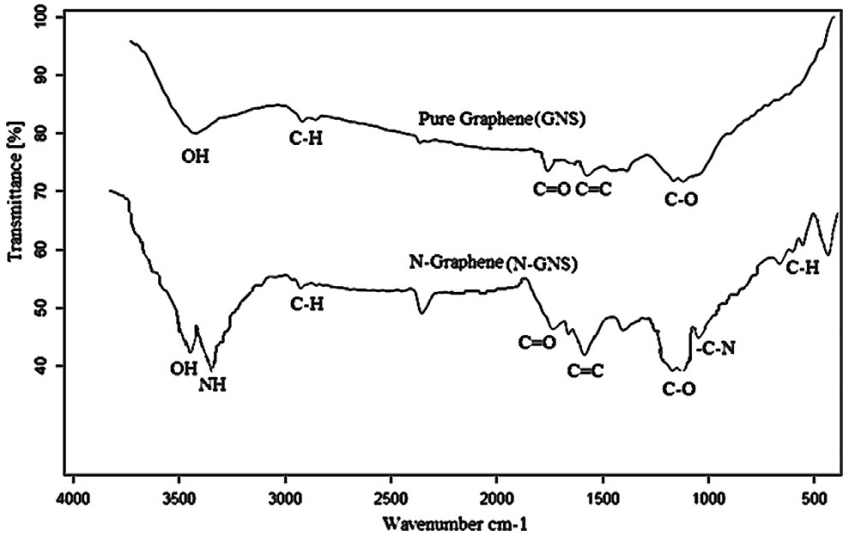

Fig. 1. FTIR spectrum of pure GNS and functionalized GNS

Raman spectra of GNS and N-GNS are shown in Fig. 2. The peaks at 1318 and 1594 cm^{-1} could be corresponded to the D and G bands of GNS and N-GNS, respectively [2]. The D peak is from the sp^3 defect sites, while the G peak is related to the bond stretching of all sp^2 carbon domains [3]. So, the ratio between the D and G peaks (D/G) shows the defect level in graphene. This ratio approaches zero for highly ordered pyrolytic graphite [4]. The D/G ratio for N-GNS (2.06) is higher than that of GNS (1.53), suggesting an increase of sp3 defect sites. This increase could be ascribed to the nitrogen functional groups [5], which would be used for the subsequent deposition of cobalt nanoparticles. These defect sites act as favorable nucleation sites for the formation of the Co-based nanoparticles that are anchored to the graphene surface. This will reduce the mobility of these particles and decrease their tendency to agglomerate.

3.2. Characterization of catalyst

The results of ICP, BET and porosity measurements for the supports and the fresh calcined and used catalysts are listed in Table 1. ICP analyses of the catalysts revealed that the metal contents of the catalysts were fairly similar and close to the targeted metal content of 15 wt% Co. According to BET results (Table 1), BET surface area for N-GNS is higher than that of pure GNS (242 vs. 216 m^2/g). The difference may be attributed to the nature and textural morphology of the functionalized GNS. 15 wt.% cobalt decreased the BET surface area for Co/GNS catalyst from 216 to 154 m^2/g. While the same loading of cobalt decreased the BET surface

area for Co/N-GNS catalyst from 242 to 210. These data indicate that pore blockage is lower in the case of Co/N-GNS catalyst, which is due to better dispersion of the cobalt particles on the functionalized support. Table 1 also shows that after 144 hrs continues FT synthesis the BET surface area of Co/GNS catalyst decreased from 150 to 137 m^2/g and the BET surface area of Co/N-GNS catalyst decreased from 210 to 194 m^2/g. In addition, the pore volume decreased from 0.63 to 0.45 cm^3/g and 0.68 to 0.61 cm^3/g, for the Co/GNS and Co/N-GNS catalysts, respectively. These values indicate that pore blockage during FT synthesis for Co/GNS catalyst is higher than that for Co/N-GNS catalyst and this is likely due to higher rates of sintering and clusters growth [6].

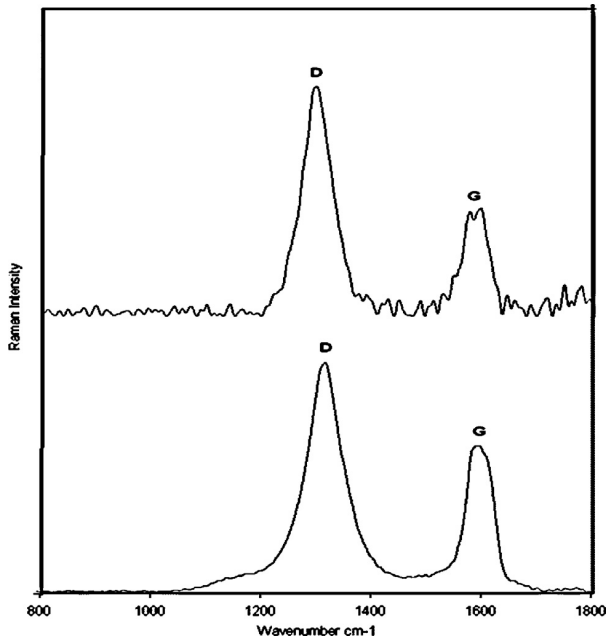

Fig. 2. Raman spectra of the GNS and functionalized GNS

Table 1. ICP, BET, Porosity and XRD data related to the catalysts

Support/catalyst	Co (wt.%)	S_{BET} (m^2/g)	Pore volume (cm^3/g)	Average pore radius (nm)	D_{XRD} (nm)
GNS	-	216	0.83	0.69	-
Fresh Co/GNS	14.89	154	0.63	0.62	12.0
Used Co/GNS	14.87	137	0.45	0.61	13.6
N-GNS	-	245	0.90	0.63	-
Fresh Co/N-GNS	15	210	0.68	0.58	10.4
Used Co/N-GNS	14.77	194	0.61	0.56	11.3

The stability of the Co/N-GNS may be attributed to the extent of functional groups which prevented metal site agglomeration or sintering, and unavailability of some active sites due to pore blockage [4]. Co nano particles dispersion and size distribution properties for fresh Co/GNS and Co/N-GNS samples were further investigated by TEM. As shown in Fig. 3, it can be seen that the Co nanoparticles are uniform while some of the particles are aggregated on the GNS. But, Co nanoparticles were much more uniform on the Co/N-GNS [7]. Meanwhile, Fig. 3 displays the histograms of Co particle size distributions obtained by measuring the sizes of about 50 randomly selected particles. As shown, the metal nano particles are better dispersed on N-GNS surface and the sizes of cobalt particles are between about 4–11 nm. While, on the GNS supported catalyst, a broader particle size distribution of Co nanoparticles is formed with particle diameters in the range of 3–15 nm. The N-GNS support enables to control a narrow cobalt nanoparticle size distribution, because the surface functional groups act as sites of interaction with metal precursor [8] and incorporation of nitrogen functional groups on

the carbon lattice is responsible the nucleation and growth mechanism of Co nano particles, leading to smaller particle size, better dispersion and narrower size distribution [7-8].

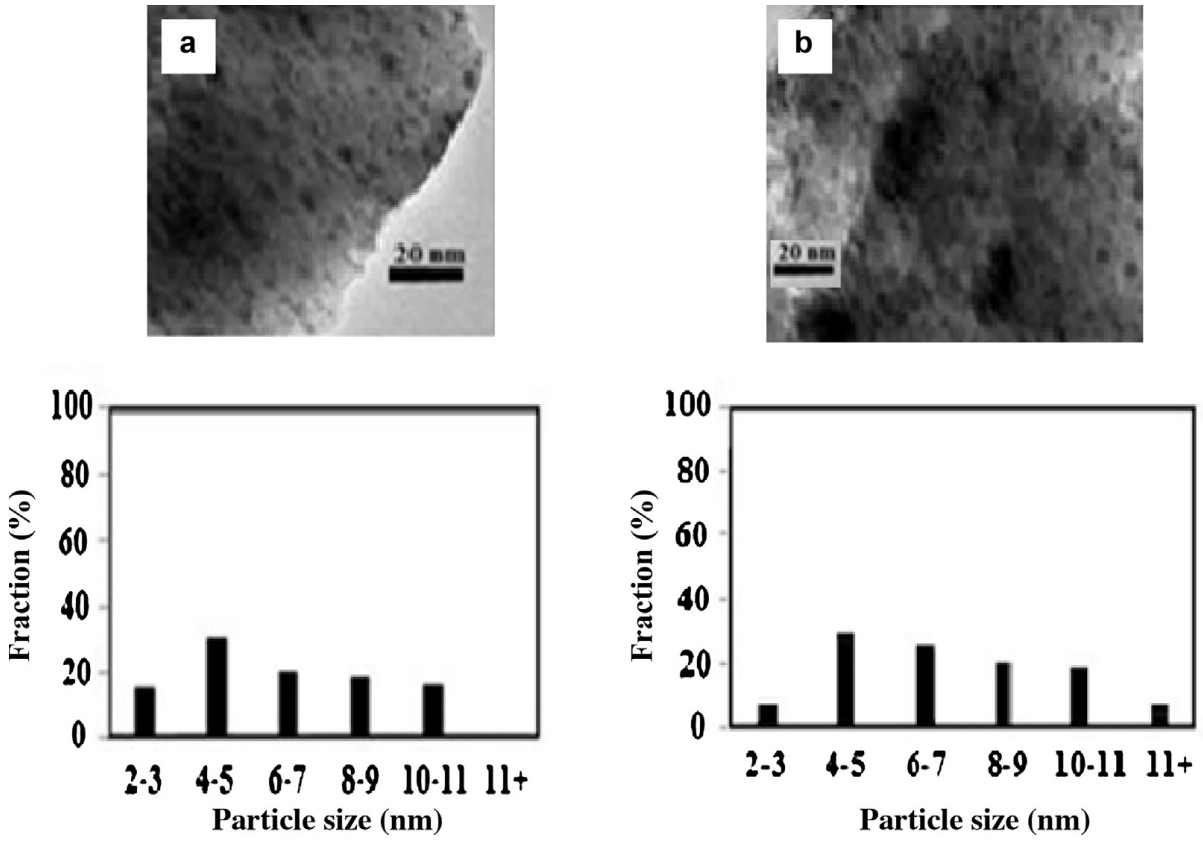

Fig. 3. TEM images of (a) fresh Co/N-GNS (b) fresh Co/GNS catalyst.

Also, according to Raman results there are more defects on N-GNS compared to GNS. These anchoring sites prevent metal particles agglomeration and sintering.

The structure and crystallinity of the fresh Co/GNS and Co/N-GNS catalysts are assessed by XRD as shown in Fig. 4. For the calcined fresh Co/GNS, the peaks at 2θ values of 25.0° and 43.0° correspond to graphite diffractions [9], while the other peaks in the patterns of Co/GNS are related to different crystal planes of Co_3O_4 and CoO. No peak was observed indicating formation of cobalt support compounds in the XRD patterns of the fresh Co/GNS. In the XRD of the fresh Co/GNS the peak at 36.8°is the most intense peak of Co_3O_4. Several studies suggest that Co_3O_4 is the active phase and other peaks, which correlate with a cubic cobalt structure has no influence on the product selectivity [8]. On the pattern of the fresh Co/N-GNS nano catalyst the peaks at 25.0° and 43.0°correspond to GNS. The peak at 36.8° is the most intense peak of Co_3O_4 nano particles. Minor peaks were also observed which correlate with a cubic structure of cobalt. As is shown, for Co/N-GNS nano catalyst, no peak is appeared indicating bulk crystalline cobalt carbide. Table 1 also shows the average Co_3O_4 particle size of the catalysts calculated from XRD patterns using Scherer formula at 2θ value of 36.8° [10]. This table indicates that the average Co_3O_4 crystallite size in Co/N-GNS is smaller than that of Co/GNS. Incorporation of nitrogen functional groups on the carbon lattice will lead to better distribution of particles, which in turn leads to lower cobalt cluster sizes. XRD patterns of the used Co/GNS and Co/N-GNS nano catalysts are also shown in Fig. 4. As is observed, the resulting patterns for the used catalysts are very complex. In the XRD pattern of the used Co/GNS, support peaks appeared at 2θ values of 25.0° and 43.0°. The peaks at 2θ values of 51.1° and 75.8° correspond to the metallic cobalt (Co°) [11]. Also the peak at 2θ value of 46.9°correlates well with Co_2C. There are a number of ways that carbon can affect the catalyst activity. The carbon

deposition may block the catalyst pores resulting in diffusion limitations, poison the metal surface by binding irreversibly or even encapsulate metal particles [12]. Subsurface carbon may also play a role in electronic inhibition of activity [13]. It has also been shown that carbon bound to a metal surface can induce a surface reconstruction which will affect the activity [14]. The diffusion of carbon into cobalt can also result in the formation of bulk cobalt carbide [15]. Bulk cobalt carbide is not active for FT reaction and results in both activity and selectivity loss, presumably through electronic inhibition that affects the dissociation of CO [16-17]. It has been shown that bulk carbide can form during conditions where hydrogen is depleted. The peaks at 2θ values of 36.8◦ and 42.5◦ correspond to Co_3O_4 and CoO. Although a fraction of cobalt clusters may be oxidized in presence of significant amount of water formed during FT synthesis with high conversions, some amount of the cobalt oxide in the used sample probably is formed during the discharge and passivation step at room temperature. In the XRD pattern of the used Co/N-GNS, similar to the corresponding pattern of the used Co/GNS, the peaks of support, metallic cobalt, cobalt oxides and cobalt carbide have been appeared at the same 2θ values but the intensities of the peaks are different. Table 1 show that 144 hrs continuous FT synthesis increased the average crystal sizes for both catalysts. However, the crystal growth was more significant in the case of Co/GNS catalyst. It seems that for Co/GNS catalyst, poor interaction with the metal particles causes further agglomeration and sintering. Functionalization and pretreatment of the support remarkably influence the interaction between cobalt and GNS. The presence of functional groups on GNS surface gives rise to cation-exchange properties which can act as anchoring sites for the metal particles and reducing agglomeration and sintering [18-19].

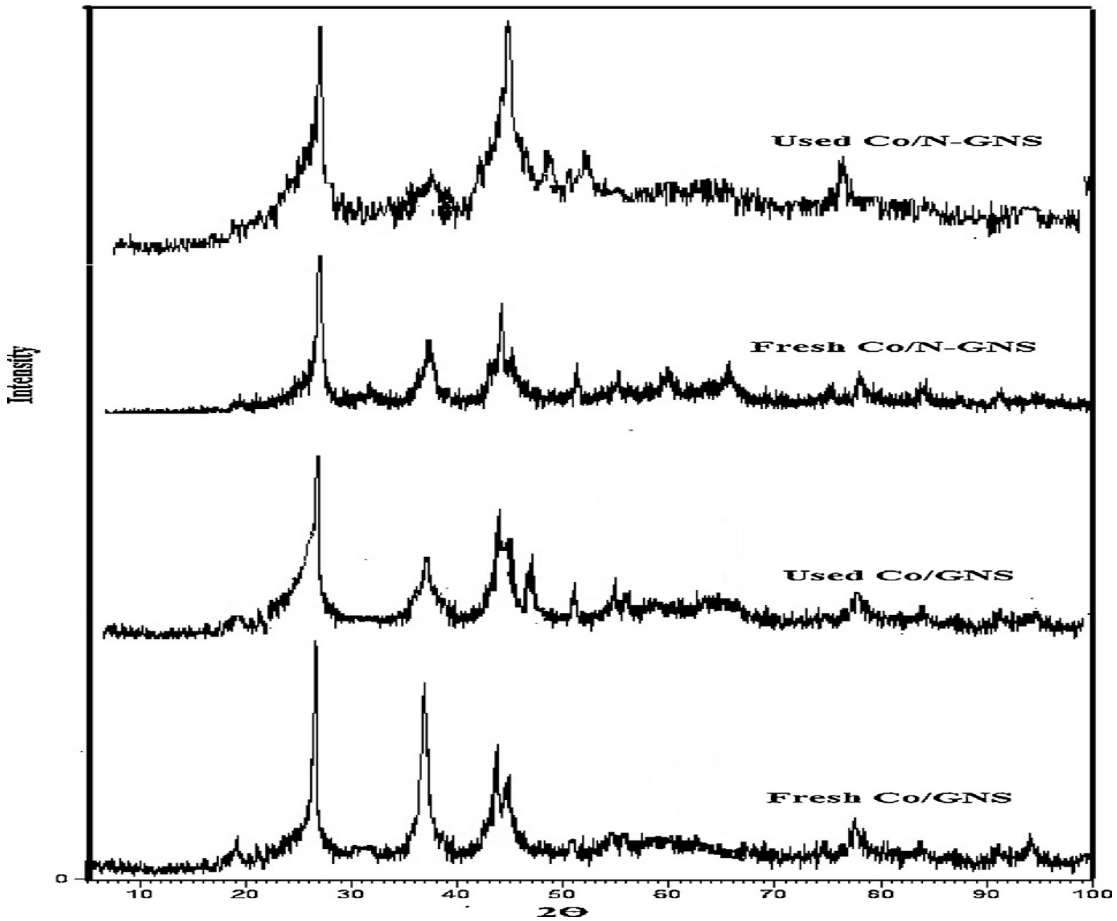

Fig. 4. XRD patterns of the fresh and used Co/GNS and Co/N-GNS catalysts.

The TPR spectra of the fresh calcined catalysts are presented in Fig. 5. The low temperature peak is typically assigned to reduction of Co_3O_4 to CoO, although a fraction of the peak likely comprises the reduction of the larger, bulk-like CoO species to Co^o [20]. The second broad peak is assigned to reduction of small CoO to Co^o species, which also includes the reduction of cobalt species that interact with the support. According to Fig. 5, functionalization of the support (Co/N-GNS catalyst) has shifted the reduction peaks to lower temperatures, indicating higher reducibility for cobalt particles deposited on functionalized GNS. TEM and XRD tests showed that the average particles size of Co/GNS catalyst is greater than that of Co/N-GNS catalyst. Large particles can be reduced easier than small particles. But, cobalt particles of Co/N-GNS catalyst are easily reduced because of the hydrogen spill-over of functional groups [21].

The broader shoulder on the TPR profile of catalysts is likely due to varying degrees of interaction of cobalt particles with support that depends on the size. The degree of interaction is higher for smaller cobalt particles [8]. It should be noted that, the area under the TPR peaks is proportional to the amount of H_2 consumed during the reduction process and percentage of catalyst reduction. The area under the TPR peaks for Co/N-GNS is 1.4 times larger than that for Co/GNS catalyst, indicating the higher degree of reduction for Co/N-GNS catalyst. Higher degrees of reduction will make more cobalt atoms to be available for FTS reaction in the Co/N-GNS catalyst in comparison with the Co/GNS catalyst. Fig. 5 also presents the TPR profiles of the used calcined Co/GNS and Co/N-GNS nano catalysts after 144 h continuous FT synthesis.

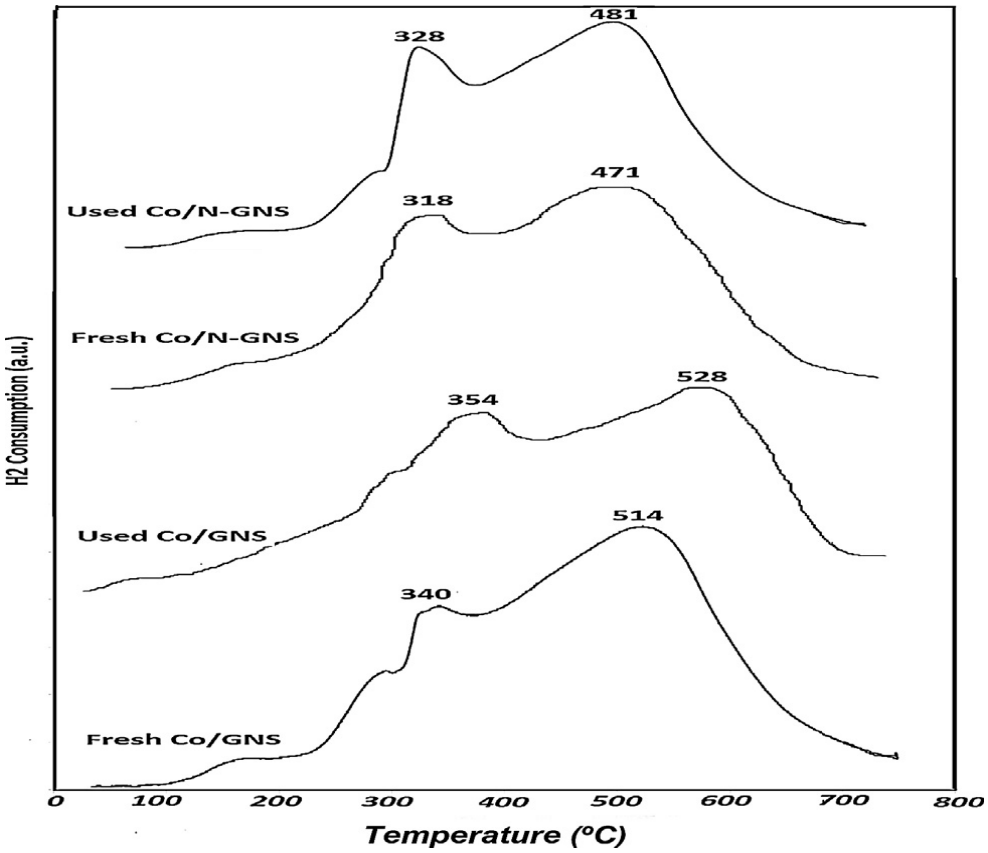

Fig. 5. TPR patterns of the fresh and used catalysts from 30 to 900 C.

As shown, the peaks of the used Co/GNS and Co/N-GNS nano catalysts shifted to higher temperatures showing that the reduction of the cobalt oxides of the used calcined catalyst occurred at higher temperatures than that of the fresh calcined Co/GNS and Co/N-GNS catalysts, indicating an increase in the degree of interaction of cobalt with the supports during FT synthesis. Also, this figure shows that 144 hrs continuous FT synthesis with both catalysts increased the tailing of the second TPR peak, which confirms the interaction of cobalt with

support during FT synthesis. XRD tests showed that the hydrocarbons can accumulate on the surface and can slowly be converted to carbon or coke. Carbon in different forms can interact and block cobalt surfaces [22]. Furthermore, this figure shows that, the area under the TPR peaks for the used Co/N-GNS is 1.46 times higher than that for the used Co/GNS catalyst.

Percentage dispersion and crystallite sizes of the cobalt particles determined by H_2-TPD and pulse reoxidation of the calcined fresh and used catalysts are given in Table 2. For each sample, dispersion and particle size were calculated based on the total amount of cobalt in the catalyst samples. The percentage of reduction was measured from the oxygen titration after H_2-TPD, assuming Co^o is reoxidized to Co_3O_4. As shown, functionalization of GNS considerably increased the hydrogen uptake and percentage dispersion. Also, the average particles diameter decreased, which are in agreement with the results of XRD and TEM tests. Also, the percentage reduction of the catalyst shows a considerable increase. Therefore, it can be concluded that functional groups play an important role on dispersion and degree of reducibility of cobalt catalyst. Higher dispersions and smaller cobalt cluster sizes in the case of the catalysts prepared by functionalized GNS will increase the number of sites available for CO conversion and hydrocarbon formation reactions rates [4].

Also, the results of H_2 chemisorption and oxygen titration tests for the used Co/GNS and Co/N-GNS nano catalysts are shown in Table 2. As shown in Table 2, the hydrogen consumption for the used Co/GNS and Co/N-GNS nano catalysts are lower than that of the fresh calcined catalysts. Both the percentage reduction and dispersion calculated based on the total cobalt decreased significantly. 144 hrs continues FT synthesis decreased the dispersion of Co/GNS nano catalyst form 23.7% to 21% and that of Co/N-GNS nano catalyst from 27.2% to 25.7%. As shown in Table 2, for Co/GNS nano catalyst, 144 hrs continuous FT synthesis increased the average cobalt nano particles diameter from 7.8 to 8.8 nm. At the same time, the average cobalt nano particles diameter of Co/N-GNS nano catalyst increased from 6.8 to 7.2 nm. These data show that the rate of sintering or cluster growth for the Co/GNS nano catalyst is much higher than that for the Co/N-GNS nano catalyst. So it can be concluded that, for the Co/GNS nano catalyst the main cause of deactivation is poor interaction with the metal particles that causes sintering or cluster growth.

Table 2. Crystallite size and %dispersion of cobalt determined by H_2 TPD and reoxidation

Catalyst	μ mole H_2 /g cat.	μ mole O_2 consumed/g cat.	%Red.	%Dispersion	dp (nm)
Fresh Co/GNS	457	298	48.31	23.7	7.8
Used Co/GNS	438	287	36.14	21	8.8
Fresh Co/N-GNS	287	375	55.6	27.2	6.8
Used Co/N-GNS	279	366	48.3	25.7	7.2

3.3. Catalysts activity and product selectivity

Table 3 and Fig. 6 show the amounts of %CO conversion, FTS rate, CO_2, CH_4, light C_2–C_4 gases and liquid C_5^+ selectivities for the Co/GNS and Co/N-GNS catalysts during the first 24 hrs FT synthesis after catalysts stabilization. As shown, the FTS rate for the Co/N-GNS catalyst (0.354 g HC/(g cat. h)) is higher than that of the Co/GNS nano catalyst (0.325 g HC/(g cat h)).

Table 3. %CO conversion, FTS rate for Co/GNS and Co/N-GNS catalysts

Catalyst	% CO conversion first 24 h	O/P	FTS rate (g CH/(g cat . h)) after 24 hrs	% CO conversion after 144 h	FTS rate (g CH/(g cat . h)) after 144 hrs
Co/GNS	78.4	1.19	0.325	74.3	0.298
Co/N-GNS	84.9	0.95	0.354	81.6	0.340

In accordance with the FTS rate, the CO conversion for Co/N-GNS is 84.9% in comparison to 78.4% for the Co/GNS catalyst. The results of catalysts characterization showed that the functionalization on GNS increases the catalyst reducibility, adsorption of hydrogen on catalyst

surface, the metal dispersion, and decreases the average cobalt particle sizes. All these effects can be evidence for increasing the number of surface active cobalt sites and as a result increasing the FTS reaction rate. Fig. 6 compares the hydrocarbon products distribution for catalysts at steady state condition during first 24 hrs. As shown in this figure, methane selectivity increased and liquid C_5^+ selectivity decreased for functionalized GNS supported catalyst. As mentioned before, functional groups will increase the amount of hydrogen adsorbed on the catalyst surface and then enhance the termination reactions to paraffin instead of chain growth to heavier hydrocarbons. The olefin to paraffin ratio for Co/GNS and Co/N-GNS catalysts were 1.19 and 0.95, respectively. Lower amount of olefin to paraffin ratio in the final products of Co/N-GNS catalyst confirms higher rate of termination reactions to paraffins.

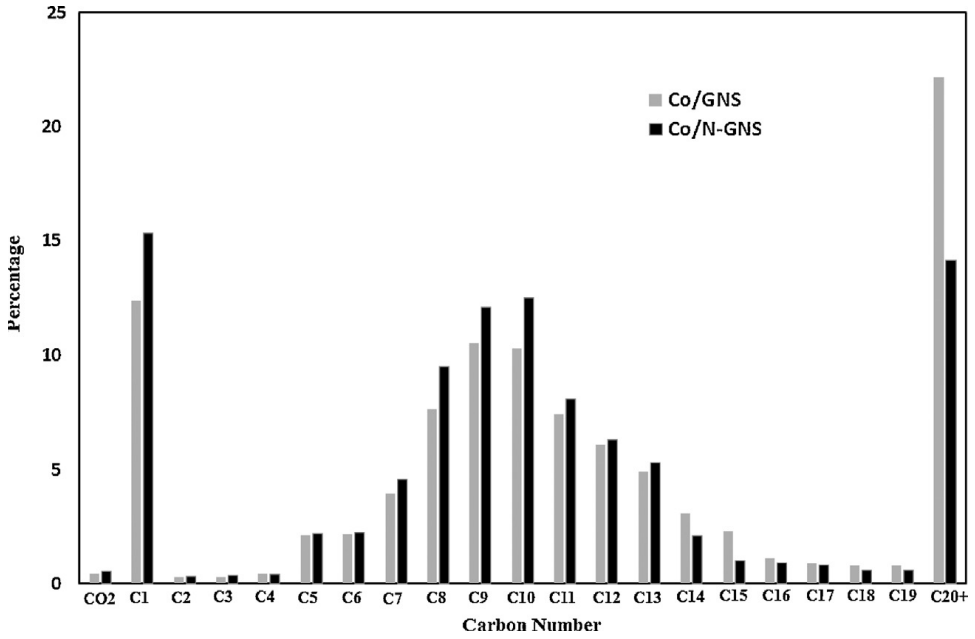

Fig. 6. Product selectivity for Co/GNS and Co/N-GNS catalysts for first 24 h (T = 220°C, P = 1.8 MPa, H_2/CO = 2)

3.4. Catalyst stability

Table 3 also, presents the variations of %CO conversion during 144 hrs continuous FT synthesis for both catalysts. It can be seen that, for both catalysts, during 144 h FT synthesis, the CO conversion considerably decreased. In the case of Co/GNS catalyst, the %CO conversion decreased from 78.4 to 74.3 (5.21% decrease). For the Co/N-GNS catalyst, the %CO conversion decreased from84.9 to 81.6 (3.88% decrease).

The rate of deactivation is higher for the Co/ GNS catalyst. The results of XRD tests (Table 1 and Fig. 4), the results of H_2chemisorption and reoxidation tests (Table 2) confirm the higher cluster growth rate during 144 hrs on stream for the Co/GNS catalyst in comparison with Co/N-GNS catalyst. They show that the catalyst supported on the functionalized GNS is more stable than the catalyst supported on the common GNS. One of the major factors for catalyst deactivation is metal site agglomeration or sintering during FT reactions. The stability of the catalyst can be attributed to the extent of functional groups and more defects and/or the structure of N-GNS support. More defects on the surface work as anchoring sites for stable metal particles on the supports surface [18]. In addition to all sources of deactivation studied in this work, the coke deposition on the catalyst surface is another important cause for cobalt catalyst deactivation. The result of XRD tests (Fig. 4) shows that the coke deposition on the Co/GNS catalyst is more than Co/N-GNS catalyst. Production of heavy unsaturated hydrocarbons during the FT synthesis can be the main source of refractory coke formation on the cobalt crystallite sites, which led to catalyst deactivation [23]. Fig. 7 shows the variations of methane and C_5^+ liquid hydrocarbons selectivity with reaction time. Fig. 7 shows that for both catalysts,

the selectivity of CH_4 decreases with time on stream during 144 hrs FT synthesis at 220 °C and 1.8 MPa. Also, Fig. 7 shows that for both catalysts the C_5^+ selectivity increases during 144 h FT synthesis. It has been shown [24] that the larger cobalt particles are more selective to higher molecular weight hydrocarbons and smaller cobalt particles are selective to methane and light gaseous hydro-carbons. It can be concluded that the sintering of smaller Co particles leads to enhancement of C_5^+ selectivity and suppression of CH_4 production with time on stream. The higher rate of sintering of the cobalt particles in the case of Co/GNS catalyst is believed to be the main reason for greater enhancement of C_5^+ selectivity and suppression of CH_4.

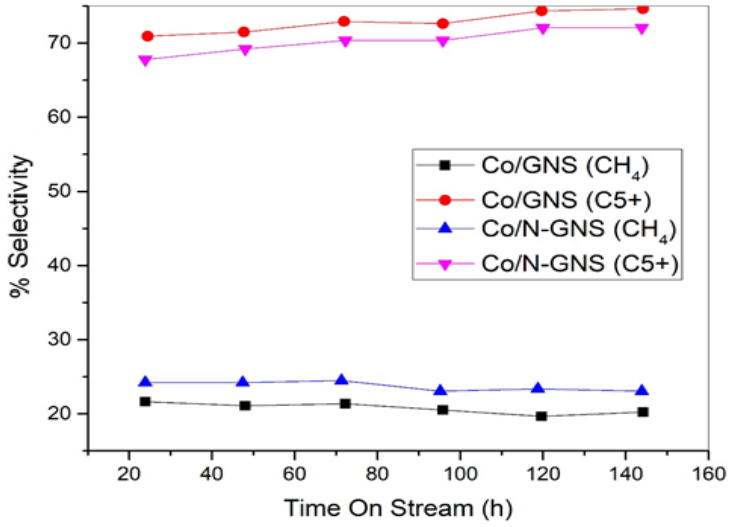

Fig. 7. Variations of methane and C_5^+ hydrocarbons selectivity with reaction time

4. Conclusion

The study has been focused on the GNS and functionalized GNS as support for cobalt catalyst to investigate the effect of support functionalization on selectivity, activity and stability of the cobalt catalyst. The catalyst was loaded on the surface of the supports by CVD method. The deposition of cobalt nanoparticles was improved in the presence of functionalized GNS. The particle size distribution was narrowed by employing functionalized GNS as support. Functionalization increased the percentage dispersion and catalyst reducibility. The catalyst activity was enhanced by GNS functionalization.

References

[1] Tavasoli A, Karimi S, Taghavi S, Zolfaghari Z, Amirfirouzkouhi H. Comparing the deactivation behaviour of Co/CNT and Co/-Al_2O_3 nano catalysts in Fischer–Tropsch synthesis. J. Nat. Gas Chem., 2012; 21 (5), 605–613.

[2] Guo S, Wen D, Zhai Y, Dong S, Wang E. Platinum nanoparticle ensemble-on-graphene hybrid nanosheet: one-pot, rapid synthesis, and used as new electrode material for electrochemical sensing. ACS Nano, 2010; 4 (7), 3959–3968.

[3] Panchakarla LS, Subrahmanyam KS, Saha SK, Govindaraj A, Krishnamurthy HR, Waghmare UV, Rao CNR. Synthesis, structure and properties of boron and nitrogen doped graphene. Adv. Mater., 2009; arXiv reprint arXiv:0902.3077.

[4] Davari M, Karimi S, Tavasoli A, Karimi A. Enhancement of activity, selectivity and stability of CNTs-supported cobalt catalyst in Fischer–Tropsch via CNTs functionalization. Appl. Catal. A: Gen., 2014; 485, 133–142.

[5] Wang S, Zhang L, Xia Z, Roy A, Chang DW, Baek JB, Dai L. BCN graphene as efficient metal-free electrocatalyst for the oxygen reduction reaction. Angew. Chem. Int. Ed., 2012; 51 (17), 4209–4212.

[6] Moussa SO, Panchakarla LS, Ho MQ, El-Shall MS. Graphene-supported, iron-based nanoparticles for catalytic production of liquid hydrocarbons from synthesis gas: the role of the graphene support in comparison with carbon nanotubes. ACS Catal., 2014; 4 (2), 535–545.
[7] Sun Q, Kim S. Synthesis of nitrogen-doped grapheme supported Pt nanoparticles catalysts and their catalytic activity for fuel cells. Electrochim. Acta, 2015; 153, 566–573.
[8] Jacobs G, Das TK, Zhang Y, Li J, Racoillet G, Davis BH. Fischer–Tropsch synthesis: support, loading, and promoter effects on the reducibility of cobalt catalysts. Appl. Catal. A: Gen., 2002; 233 (1), 263–281.
[9] Subrahmanyam KS, Vivekchand SRC, Govindaraj A, Rao CNR. A study of graphenes prepared by different methods: characterization, properties and solubilization. J. Mater. Chem., 2008; 18 (13), 1517–1523.
[10] Bechara R, Balloy D, Vanhove D. Catalytic properties of Co/Al_2O_3 system for hydrocarbon synthesis. Appl. Catal. A: Gen., 2001; 207 (1), 343–353.
[11] Karimi S, Tavasoli A, Mortazav, Y, Karimi A. Enhancement of cobalt catalyst stability in Fischer–Tropsch synthesis using graphene nanosheets as catalyst support. Chem. Eng. Res. Des., 2015; 104, 713–722.
[12] Bartholomew CH. Mechanisms of catalyst deactivation. Appl. Catal. A: Gen., 2001; 212 (1), 17–60.
[13] Zonnevylle MC, Geerlings JJC, van Santen RA. Conversion of surface carbidic to subsurface carbon on cobalt (0001): a theoretical study. Surf. Sci., 1990; 240 (1–3), 253–262.
[14] Ciobîca IM, van Santen RA, van Berge PJ, van de Loosdrecht J. Adsorbate induced reconstruction of cobalt surfaces. Sur. Sci.,2008; 602 (1), 17–27.
[15] Hofer LJE, Peebles WC. Preparation and X-ray diffraction studies of a new cobalt carbide. J. Am. Chem. Soc., 1947; 69 (4), 893–899.
[16] Weller S, Hofer LJE, Anderson RB. The role of bulk cobalt carbide in the Fischer–Tropsch synthesis1. J. Am. Chem. Soc. , 1948; 70 (2), 799–801.
[17] Xiong J, Ding Y, Wang T, Yan L, Chen W, Zhu H, Lu Y. The formation of Co_2C species in activated carbon supported cobalt-based catalysts and its impact on Fischer–Tropsch reaction. Catal. Lett., 2005; 102 (3–4), 265–269.
[18] Zhang Y, Liu Y, Yang G, Endo Y, Tsubaki N. The solvent effects during preparation of Fischer–Tropsch synthesis catalysts: improvement of reducibility, dispersion of supported cobalt and stability of catalyst. Catal. Today, 2009; 142 (1), 85–89.
[19] Fu T, Liu R, Lv J, Li Z. Influence of acid treatment on N-doped multi-walled carbon nanotube supports for Fischer–Tropsch performance on cobalt catalyst. Fuel Process. Technol., 2014; 122, 49–57.
[20] Trépanier M, Dalai AK, Abatzoglou N. Synthesis of CNT-supported cobalt nanoparticle catalysts using a microemulsion technique: role of anoparticle size on reducibility, activity and selectivity in Fischer–Tropsch reactions. Appl. Catal. A: Gen., 2010; 374 (1), 79–86.
[21] Chen W, Fan Z, Pan X, Bao X. Effect of confinement in carbon nanotubes on the activity of Fischer–Tropsch iron catalyst. J. Am. Chem. Soc., 2008; 130 (29), 9414–9419.
[22] Rytter E, Holmen A. Deactivation and regeneration of commercial type Fischer–Tropsch cocatalysts—a mini-review. Catalysts, 2015; 5 (2), 478–499.
[23] Tavasoli A, Sadagiani K, Khorashe F, Seifkordi AA, Rohani AA, Nakhaeipour A. Cobalt supported on carbon nanotubes—a promising novel Fischer–Tropsch synthesis catalyst. Fuel Process. Technol., 2008; 89 (5), 491–498.
[24] Velasco JA, Lopez L, Cabrera S, Boutonnet M, Järås S. Synthesis gas production for GTL applications: thermodynamic equilibrium approach and potential for carbon formation in a catalytic partial oxidation pre-reformer. J. Nat. Gas Sci. Eng., 2014; 20, 175–183.

To whom correspondence should be addressed: Iraj Kazemnejad, Department of Chemistry, Central Tehran Branch, Islamic Azad University, Tehran, Iran, E-mail: kazemnejad.i@gmail.com